Available online at ScienceDirect

ScienceDirect

J. Mater. Sci. Technol., 2014, 30(1), 77−89

JMST

www.JMST.org

Lactobionic Acid as a New Synergist in Combination with Phosphonate−Zn(II) System for Corrosion Inhibition of Carbon Steel

S. Srinivasa Rao[1)*], *B.V. Appa Rao*[2)], *S. Roopas Kiran*[3)], *B. Sreedhar*[4)]

1) Department of Chemistry, V. R. Siddhartha Engineering College (Autonomous), Vijayawada 520007, Andhra Pradesh, India
2) Department of Chemistry, National Institute of Technology Warangal (NITW), Warangal 506004, Andhra Pradesh, India
3) INFN, Sezione di Padova, Via Marzolo 8, 35131 Padova, Italy
4) Inorganic & Physical Chemistry Division, Indian Institute of Chemical Technology (IICT), Hyderabad 500007, Andhra Pradesh, India

[Manuscript received April 8, 2012, in revised form October 17, 2012, Available online 10 October 2013]

Studies on lactobionic acid introduced as a synergist in the presence of phosphonobutane-1,2,4-tricarboxylic acid (PBTC) and zinc ions for corrosion control of carbon steel in aqueous environment are presented. The investigations revealed that lactobionic acid (LBA) acts as an excellent synergist in corrosion inhibition. Optimum concentrations of all the three components of the ternary formulation are established by gravimetric studies. Potentiodynamic polarization studies indicate that the new ternary system is a mixed inhibitor. Impedance studies show that a protective film is formed on the metal surface in the presence of the inhibitor formulation. The film is found to exhibit its protective nature even at higher temperatures up to 60 °C. Analysis of the protective film by X-ray photoelectron spectroscopy (XPS) and reflection absorption Fourier transform infrared (FTIR) spectroscopy infers the presence of $Zn(OH)_2$, oxides and hydroxides of iron and the inhibitor molecules in the surface film probably in the form of a complex, [Zn(II)−PBTC−LBA]. The morphological studies by scanning electron microscopy (SEM) and the topographical studies by atomic force microscopy (AFM) also indicate the presence of protective film on the metal surface. A plausible mechanism of corrosion inhibition is proposed.

KEY WORDS: Corrosion inhibitor; Carbon steel; Synergism; X-ray photoelectron spectroscopy; Electrochemical impedance spectroscopy

1. Introduction

Phosphonate−Zn^{2+} systems are prominent inhibitors for corrosion control of carbon steel in cooling water systems. Synergistic effect existing between phosphonic acids and zinc ions on corrosion inhibition of carbon steel has been studied[1−7]. The reports pointing to synergistic action of phosphonates and Zn^{2+} explained that the inhibiting action is due to the formation of protective films on metal surface[2]. It was also reported that phosphonates act anodically and form complexes with metal ions while zinc ions act cathodically and form $Zn(OH)_2$ resulting in the synergistic corrosion inhibition[8]. Although phosphonate−Zn^{2+} formulations are highly effective in corrosion control of carbon steel, they require high levels of both Zn^{2+} and phosphonate. But, the disposal of zinc salts in wastewater at higher levels has become unacceptable. The permissible limit of zinc ions in water is about 2 mg dm^{-3} Ref. [9]. Owing to these strict environmental restrictions on industrial wastewater disposal, researches have been progressed in the direction to minimize the concentration of Zn^{2+} in the inhibitor formulations. An effective method to handle this task is to add another non-toxic component of either organic or inorganic nature, which can synergistically act along with phosphonate and Zn^{2+} and bring about effective corrosion inhibition at relatively lower concentrations of zinc ions. A few of such ternary inhibitor formulations were reported in literature[10−13].

In this study, a new environmentally friendly ternary inhibitor formulation with relatively low concentrations of both phosphonate and Zn^{2+} in the presence of an organic compound has been proposed. The selected phosphonic acid and the organic compound are 2-phosphonobutane-1,2,4-tricarboxylic acid (PBTC) and lactobionic acid (LBA), respectively. PBTC consists of a phosphonic acid group and three carboxylic acid groups. The oral and dermal toxicities of PBTC, as tested in rats have been found to be very low[14]. The ecological risk for aquatic organisms has been reported to be the lowest for PBTC among several phosphonates studied[14]. Therefore, this compound is

* Corresponding author. Tel.: +91 8897557599; Fax: +91 870 2459547; E-mail address: ssrnitw@gmail.com (S.S. Rao).

http://dx.doi.org/10.1016/j.jmst.2013.10.003

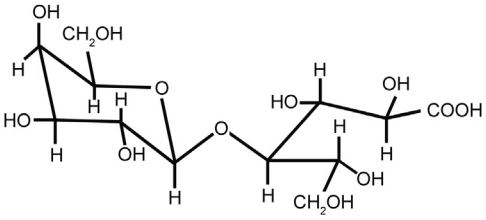

Fig. 1 Molecular structure of lactobionic acid (LBA).

environmentally friendly. Bohnsack et al. inferred that phosphonocarboxylic acids, like PBTC, are able to prevent precipitation of $Fe(OH)_3$[15]. Lactobionic acid (4-O-β-D-galactopyranosylgluconic acid) is the oxidation product of disaccharide lactose and is reported to be biodegradable and non-toxic compound[16]. It contains eight hydroxyl groups and one carboxyl group and has the complexing ability with metal ions[17]. To our knowledge, LBA was not so far reported to be a synergist to any phosphonate-based corrosion inhibitor formulation. The main objective of the present study is to investigate the synergistic action of the selected compounds namely PBTC, Zn^{2+} and LBA in the corrosion control of carbon steel in nearly neutral aqueous chloride environment. For the present study, 200 mg L^{-1} of NaCl solution has been chosen because of the following reason. The water used in cooling water systems is generally either demineralized water or unpolluted surface water. In either case, the aggressiveness of the water will never exceed that of 200 mg L^{-1} of NaCl.

2. Experimental

2.1. Solutions and specimens

For all the studies, the specimens taken from a single sheet of carbon steel with the following composition were chosen: C 0.1%−0.2%, P 0.03%−0.08%, S 0.02%−0.03%, Mn 0.4%−0.5% and the balance iron. Prior to the tests, the specimens were polished to mirror finish with 1/0, 2/0, 3/0 and 4/0 emery polishing papers, respectively, washed with distilled water, degreased with acetone and dried. For gravimetric measurements, the polished specimens with the dimensions of 3.5 cm × 1.5 cm × 0.2 cm were used while for other studies, the dimensions of the specimens are 1.0 cm × 1.0 cm × 0.1 cm. PBTC ($C_7H_{11}O_9P$), Zinc sulphate ($ZnSO_4 \cdot 7H_2O$), lactobionic acid ($C_{12}H_{22}O_{12}$) and other reagents were analytical grade chemicals. Molecular structure of lactobionic acid (LBA) is shown in Fig. 1. All the solutions were prepared with triple distilled water. The pH values of the solutions were adjusted by using 0.01 N NaOH and 0.01 N H_2SO_4 solutions. An aqueous solution consisting of 200 mg L^{-1} of NaCl has been used as the control solution throughout the study.

2.2. Gravimetric measurements

In all the gravimetric experiments, the polished specimens were weighed and immersed in duplicate, in 100 mL control solution in the absence and presence of inhibitor formulations of different concentrations, for a period of seven days. Then the specimens were reweighed after washing, degreasing and drying. During the studies, only those results were taken into consideration, in which the difference in the weight-loss of the two specimens immersed in the same solution did not exceed 0.1 mg. Accuracy in weighing up to 0.01 mg and in surface area measured up to 0.1 cm^2, as recommended by ASTM G31, was followed[18]. The immersion period of seven days was fixed in view of the considerable magnitude of the corrosion rate obtained in the absence of any inhibitor after this immersion period. The immersion period was maintained accurately up to 0.1 h in view of the lengthy immersion time of 168 h. Under these conditions of accuracy, the relative standard error in corrosion rate determinations is of the order of 2% or less for an immersion time of 168 h[19]. Corrosion rates (CR) of carbon steel in the absence and presence of various inhibitor formulations are expressed in mmpy. Inhibition efficiencies (IE_g) of the inhibitor formulations were calculated by using the formula,

$$IE_g(\%) = 100\left[(CR)_o - (CR)_I\right]/(CR)_o \quad (1)$$

where $(CR)_o$ and $(CR)_I$ are the corrosion rates in the absence and presence of inhibitor, respectively.

Gravimetric studies of the ternary formulations containing PBTC (20−40 mg L^{-1}), Zn^{2+} (10−20 mg L^{-1}) and LBA (10−70 mg L^{-1}) were carried out at pH 7. The selected concentration ranges of both PBTC and Zn^{2+} in these studies are based on the results of gravimetric studies of the binary inhibitor system, PBTC−Zn^{2+}[13]. The influence of pH on inhibition efficiency of the effective ternary inhibitor formulations was also studied in the pH range, 4−9. Gravimetric experiments were also conducted using the specimens covered by the protective film in the ternary inhibitor formulation, in order to decide the required minimum dosage of each of the components for maintenance of the protective film in the chosen corrosive environment.

2.3. Electrochemical studies

Both the potentiodynamic polarization studies and electrochemical impedance spectroscopic (EIS) studies were carried out by using the Electrochemical Workstation Model IM6e, Zahner-elektrik, GmbH, Germany and the experimental data were analyzed by using the Thales software. The measurements were conducted in a conventional three-electrode cylindrical glass cell with platinum electrode as auxiliary electrode and Ag/AgCl as reference electrode. The working electrode was carbon steel embedded in epoxy resin of polytetrafluoroethylene so that the flat surface of 1 cm^2 was the only surface exposed to the electrolyte. The three-electrode set up was immersed in control solution of 500 mL both in the absence and presence of various inhibitor formulations and allowed to attain a stable open circuit potential (OCP). The pH values of the solutions were adjusted to 7.0 and the solutions were unstirred during the experiments.

Polarization curves were recorded in the potential range of −1000 to +200 mV with a resolution of 2 mV. The curves were recorded in the dynamic scan mode with a scan rate of 2 mV s^{-1} in the current range of −20 mA to +20 mA. The ohmic drop compensation has been made during the studies. The corrosion potential (E_{corr}), corrosion current (I_{corr}), anodic Tafel slope (β_a) and cathodic Tafel slope (β_c) were obtained by extrapolation of anodic and cathodic regions of the Tafel plots. The inhibition efficiency (IE_p) values were calculated from I_{corr} values using the equation[20],

$$IE_p(\%) = \left[1 - \left(I'_{corr}/I_{corr}\right)\right] \times 100 \quad (2)$$

where I_{corr} and I'_{corr} are the corrosion current densities in the case of control and inhibited solutions, respectively.

Electrochemical impedance spectra in the form of Nyquist plots were recorded at OCP in the frequency range from 60 kHz to 10 mHz with 4−10 steps per decade. A sine wave, with 10 mV amplitude, was used to perturb the system. The impedance parameters viz., charge transfer resistance (R_{ct}), constant phase element (CPE) and CPE exponent (n) were obtained from the Nyquist plots. The inhibition efficiencies (IE_i) were calculated using the following equation,

$$IE_i(\%) = 100\left[1 - \left(R_{ct}/R'_{ct}\right)\right] \quad (3)$$

where R_{ct} and R'_{ct} are the charge transfer resistance in the absence and presence of the inhibitor, respectively. In order to study the effect of immersion period, the three-electrode set up was kept undisturbed for 24 h and impedance spectra were recorded at various immersion periods of 1 h, 6 h, 12 h and 24 h. In order to conduct the tests at various temperatures, the working electrode was immersed in the environment for 24 h at 30 °C to ensure the formation of the protective film. The Nyquist plots were then recorded at higher temperatures up to 60 °C. The temperature of the cell was controlled by using thermostat arrangement, with an accuracy of ±0.1 °C.

2.4. Surface analysis by X-ray photoelectron spectroscopy

X-ray photoelectron spectroscopy (XPS) measurements of the surface films were carried out with a Kratos analytical photoelectron spectrometer model AXIS 165 with monochromated Al$K\alpha$ X-ray source (1486.6 eV) operated at 100 W. Both the survey spectra and deconvolution spectra were recorded at four spots on each specimen. The average of the four measurements is reported. The spectra were collected at an electron take-off angle of 90°. Analyser pass energy was 80 eV, with a step of 1 eV. Deconvolution spectra were recorded with analyser pass energy of 80 eV, with a step of 0.1 eV for the elements of interest namely Fe 2p, O 1s, P 2p, C 1s and Zn 2p. Binding energies for the deconvolution spectra were corrected individually for each measurement set, based on a value of 285.0 eV for the C−C component of C 1s.

2.5. Fourier transform infrared spectroscopic studies

Fourier transform infrared (FTIR) spectra were recorded using an FTIR spectrophotometer (Thermo Electron Corporation, USA, model Nexus 670) with a resolving power of 0.125 cm^{-1}. The detector is temperature stabilised DTGS (KBr window) and liquid nitrogen cooled MCT-A and the beam splitter is XT-KBr. FTIR spectra of pure PBTC and pure LBA were recorded using the KBr pellet method. The reflection absorption FTIR spectra of the surface films were recorded in the wave number range of 4000−400 cm^{-1}. The measurements were made at a grazing angle of 85°.

2.6. Surface morphological and topographical studies

The surface morphology was observed by scanning electron microscopy (SEM) and topographical studies were carried out by atomic force microscopy (AFM). SEM images were recorded using FEI Quanta FEG 200 High Resolution Scanning Electron Microscope for the specimens immersed in the control as well as in the inhibitor solution at two different magnifications. AFM topographical images were realised using a Dimension 3100 (Nanoscope-IV) atomic force microscope in contact mode with commercial Si_3N_4 cantilever.

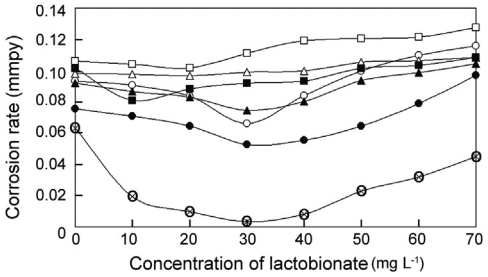

Fig. 2 Corrosion rate of carbon steel as a function of concentration of LBA added to various combinations of PBTC and Zn^{2+} at pH 7: PBTC (20 mg L^{-1}) + Zn^{2+} (10 mg L^{-1}); PBTC (30 mg L^{-1}) + Zn^{2+} (10 mg L^{-1}); PBTC (40 mg L^{-1}) + Zn^{2+} (10 mg L^{-1}); PBTC (20 mg L^{-1}) + Zn^{2+} (15 mg L^{-1}); PBTC (30 mg L^{-1}) + Zn^{2+} (15 mg L^{-1}); PBTC (40 mg L^{-1}) + Zn^{2+} (15 mg L^{-1}); PBTC (20 mg L^{-1}) + Zn^{2+} (20 mg L^{-1}).

3. Results and Discussion

3.1. Gravimetric studies

The results of gravimetric studies using the binary inhibitor formulation, PBTC−Zn^{2+}, were presented elsewhere[13] by the authors of the present study. These results indicated that the required minimum concentrations of PBTC and Zn^{2+} for the highest inhibition efficiency of 98% are 40 mg L^{-1} each, corresponding to the molar ratio of [PBTC]/[Zn^{2+}] as 1:4.4. The inhibition efficiency is due to synergistic action between PBTC and Zn^{2+} at their optimum concentrations. Lactobionic acid can form chelate-type coordination compounds with various metal ions[17,21]. When lactobionate is added as another additive to the mixture of PBTC and Zn^{2+} at relatively low concentrations of each, corrosion rate of carbon steel is reduced significantly. Hence, the ternary inhibitor formulations containing 20−40 mg L^{-1} of PBTC and 10−20 mg L^{-1} of Zn^{2+} are considered along with LBA (10−70 mg L^{-1}). The results of corrosion rates are shown in Fig. 2. None of the formulations containing 10 or 15 mg L^{-1} of Zn^{2+} showed inhibition efficiency >35% even when the concentrations of PBTC and LBA are increased to 40 mg L^{-1} and 70 mg L^{-1}, respectively. In order to achieve inhibition efficiency >95%, the required minimum concentrations of PBTC and Zn^{2+} are 20 mg L^{-1} each only corresponding to 0.75×10^{-4} mol/L and 3.1×10^{-4} mol/L, respectively, in the presence of LBA. While the binary system consisting of 20 mg L^{-1} each of PBTC and Zn^{2+} showed an inhibition efficiency of only 22%, the ternary inhibitor system containing 30 mg L^{-1} of LBA and 20 mg L^{-1} each of PBTC and Zn^{2+}, afforded an inhibition efficiency of 96%. The synergistic effect of LBA in the ternary system is established by this result. However, at higher concentrations of LBA such as 60 mg L^{-1} and 70 mg L^{-1}, the inhibition efficiency is reduced to 61% and 44%, respectively. It can be observed from Fig. 2 that in the case of all the ternary inhibitor formulations, as the concentration of LBA is increased, the corrosion rate decreases, reaches a

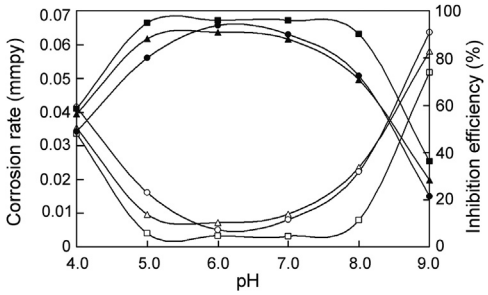

Fig. 3 Corrosion rate (CR) of carbon steel and inhibition efficiency (IE) of the ternary inhibitor formulation, PBTC (20 mg L^{-1}) + Zn^{2+} (20 mg L^{-1}) + LBA, as a function of pH at various concentrations of LBA 20 mg L^{-1}: CR —△— IE —▲—, 30 mg L^{-1}: CR —□— IE —■—, 40 mg L^{-1}: CR —○— IE —●—.

minimum at an optimum concentration of LBA and then increases. Thus, in the case of the ternary inhibitor formulation also, the mixture containing optimum concentrations of each of the components gives the highest inhibition efficiency. In other words, optimum amounts of each of the three components must be available in the solution, so that each one of them plays its own synergistic role in the formation of protective film covering the entire metal surface. It may be mentioned here that the molar ratio of PBTC:Zn^{2+}:LBA is 1.00:4.13:1.13 to exhibit excellent synergism with an efficiency of 96%.

The influence of pH on corrosion rates of carbon steel in the presence of the ternary inhibitor system and the inhibition efficiencies of the inhibitor namely, PBTC (20 mg L^{-1}) + Zn^{2+} (20 mg L^{-1}) + LBA (20−40 mg L^{-1}), in the pH range 4.0−9.0 are shown in Fig. 3. The highest inhibition efficiency could be obtained by the formulation containing PBTC (20 mg L^{-1}) + Zn^{2+} (20 mg L^{-1}) + LBA (30 mg L^{-1}) in the pH range, 5−8. But, when the pH is decreased from 5.0 to 4.0, the inhibition efficiency is reduced to 58.5% and when the pH is increased from 8.0 to 9.0, the inhibition efficiency is reduced to 36%. The reasons for the decrease of inhibition efficiency in more alkaline and more acidic environments are explained under the mechanistic aspects. Once, the protective film is formed on the metal surface by using the ternary inhibitor system consisting of PBTC (20 mg L^{-1}), Zn^{2+} (20 mg L^{-1}) and LBA (30 mg L^{-1}), the concentrations of each of these components in the inhibitor could be even less in order to maintain the protective film. The results of gravimetric studies carried out in order to determine the minimum concentrations of the formulation for maintenance of the protective film are shown in Table 1. These results show that the inhibitor mixture containing only 10 mg L^{-1} of PBTC, 10 mg L^{-1} of Zn^{2+} and 20 mg L^{-1} of LBA could maintain the protective film. The molar ratio of PBTC:Zn^{2+}:LBA in the maintenance dosage is 1.00:4.13:1.51.

Table 1 Results of gravimetric studies of the inhibitor formulations for maintenance of the protective film

Inhibitor formulation for maintenance of the film (mg L^{-1})			Corrosion rate (mmpy)	Inhibition efficiency (%)
[PBTC]	[Zn^{2+}]	[LBA]		
–	–	–	0.08108	–
20	20	30	0.00320	96.05
20	15	30	0.00538	93.36
20	10	30	0.00599	92.61
20	5	30	0.04955	38.89
15	10	30	0.00603	92.55
10	10	30	0.00682	91.58
5	10	30	0.06427	20.73
10	10	25	0.00692	91.46
10	10	20	0.00729	91.00
10	10	15	0.06496	19.87
10	10	10	0.06933	14.49
10	10	5	0.07917	2.35

3.2. Potentiodynamic polarization studies

The potentiodynamic polarization curves for carbon steel electrode in 200 mg L^{-1} NaCl solution at pH 7 in the absence and presence of various inhibitor formulations are shown in Fig. 4. The values of the electrochemical kinetic parameters namely E_{corr}, I_{corr}, β_a and β_c and the inhibition efficiency values calculated from corrosion current density are summarized in Table 2. When the possible binary combinations are studied, it was observed that they can affect the kinetics of both the anodic (dissolution of iron) and cathodic (oxygen reduction) reactions to the considerable extent. It can be observed from Fig. 4 that all the possible binary combinations shifted the corrosion potential in the cathodic direction. The figure also indicates that in the presence of all the binary combinations, there is a marked decrease in cathodic current density values. It shows that the binary combinations, although affect both the electrode reactions, can control the cathodic reaction to a greater extent. This inference is also supported by the greater shifts in cathodic Tafel slopes when compared with the shifts in anodic Tafel slopes (Table 2). Among all the possible binary combinations, the formulation containing PBTC and Zn^{2+} decreased the I_{corr} to a greater extent, corresponding to an inhibition efficiency of 66%. This is due to the fact that phosphonates in combination with Zn^{2+} exhibit good synergism in corrosion control of carbon steel[1−7]. It was reported that when the concentrations of both PBTC and Zn^{2+} are increased to 40 mg L^{-1} each, the inhibition efficiency increased to 91%[13]. It is interesting to note that such an effective inhibition could also be achieved in the present study by the addition of 30 mg L^{-1} of LBA to the combination of PBTC and Zn^{2+} at the concentration of only 20 mg L^{-1} each. When the ternary inhibitor formulation, PBTC (20 mg L^{-1}) + Zn^{2+} (20 mg L^{-1}) + LBA (30 mg L^{-1}), is considered, the shift in E_{corr} is found to be as high as 120 mV in the cathodic direction (Fig. 5). Although there are shifts in both β_a and β_c, the shift in β_c is much greater. The decrease in cathodic current density is more in comparison with that in anodic current density in the presence of the ternary inhibitor formulation. I_{corr} value is found to be minimum for the ternary inhibitor formulation among all the formulations considered for polarization studies. Hence, it can be concluded that the ternary inhibitor system retards both the anodic dissolution of carbon steel and oxygen reduction at cathodic sites in the corrosion process, its cathodic action being more pronounced. Similar phosphonate-based formulations were reported to be mixed type inhibitors[8,13,22−24]. The polarization studies also infer the synergistic action of PBTC, Zn^{2+} and LBA in corrosion control of carbon steel. This inference is supported by the inhibition efficiency values obtained from gravimetric studies.

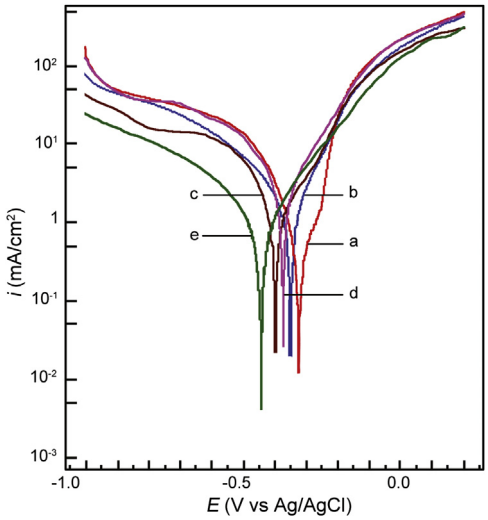

Fig. 4 Potentiodynamic polarization curves for carbon steel in 200 mg L^{-1} NaCl environment in the absence and presence of various inhibitor components: (a) no inhibitor; (b) PBTC (20 mg L^{-1}) + Zn^{2+} (20 mg L^{-1}); (c) PBTC (20 mg L^{-1}) + LBA (30 mg L^{-1}); (d) Zn^{2+} (20 mg L^{-1}) + LBA (30 mg L^{-1}); (e) PBTC (20 mg L^{-1}) + Zn^{2+} (20 mg L^{-1}) + LBA (30 mg L^{-1}).

3.3. Electrochemical impedance studies

3.3.1. Synergistic effect. Nyquist plots for carbon steel immersed in 200 mg L^{-1} of NaCl solution at pH 7 in the absence and presence of the possible binary combinations and the ternary inhibitor formulation are shown in Fig. 5. In the case of the control as well as in the presence of various formulations, the Nyquist plots are found to be depressed semicircles instead of ideal semicircles. The plots show one capacitive loop with single time constant. A capacitive loop represents the phenomenon associated with electrical double layer and arises from the time constant of the electrical double layer and charge transfer resistance. The capacitive loop corresponds to the charge transfer reaction, which depends either on direct electron transfer at the metal surface or on the electron conduction through the film surface. The depressed nature of the loop is due to the surface inhomogeneity of structural or interfacial origin, such as those found in adsorption processes[25]. In such cases, the parallel network charge transfer resistance−double layer capacitance (R_{ct}−C_{dl}) is a poor approximation especially for systems where an efficient inhibitor is present. Hence, the constant phase element (CPE) is introduced in the circuit instead of a pure double layer capacitor to give more accurate fit[26,27]. The impedance function of a CPE has the following equation[28]:

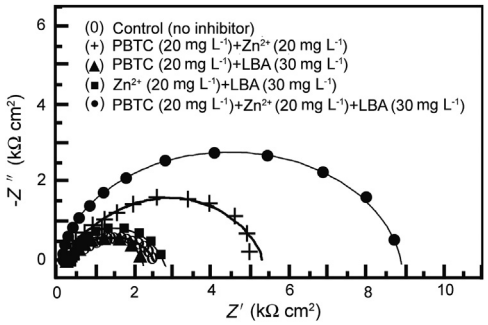

Fig. 5 Nyquist plots for carbon steel in 200 mg L^{-1} NaCl environment in the absence and presence of different combinations of the inhibitor (lines represent fitted curves).

$$Z_{CPE} = A^{-1}(i\omega)^{-n} \quad (4)$$

where A is the CPE constant, ω is the angular frequency in rad/s, $i^2 = 1$ is the imaginary number and n is a CPE exponent which can be used as a gauge of the heterogeneity or roughness of the surface[29]. Depending on the value of n, CPE can represent resistance ($n = 0$, $A = R$), capacitance ($n = 1$, $A = C$) or inductance ($n = -1$, $A = L$).

The equivalent electrical circuit model shown in Fig. 6 fits the experimental data obtained from Nyquist plots in the present study. Such an equivalent circuit was also discussed by several researchers[30−33], who obtained similar semicircles with single time constant. The impedance parameters viz., R_{ct}, CPE and CPE exponent (n) obtained from the Nyquist plots and the calculated inhibition efficiency (IE_i) values are shown in Table 3. Charge transfer resistance (R_{ct}) and the non-ideal capacitance (CPE) are the two important parameters related to corrosion processes at the metal/solution interface. The former is directly related to the rate of corrosion reaction at the interface while the latter to the structure of electrical double layer at the interface. During corrosion inhibition by the adsorption of inhibitor molecules, high R_{ct} values can be obtained due to slower corroding system[34,35]. Consequently, decrease in CPE can result from the decrease of the local dielectric constant and/or from the increase of thickness of electrical double layer, which suggests an adsorption of the inhibitor molecules on the metal surface[36]. Hence, for an effective inhibition process, there will be an increase in R_{ct} and decrease in CPE. However, there are inhibition processes that are associated with increase in capacitance values. This can be interpreted due to the replacement of water molecules in the interface by ionic inhibitor species and/or due to oxides/hydroxides of metal formed due to initial corrosion. Bonnel et al. studied corrosion of carbon steel in neutral chloride solution by impedance technique[37]. They obtained high

Table 2 Tafel parameters for carbon steel in 200 mg L^{-1} NaCl environment in the absence and presence of inhibitor formulations

Concentration (mg L^{-1})			Tafel parameters				Inhibition efficiency, IE_p (%)
PBTC	Zn^{2+}	LBA	E_{corr} (mV) vs. Ag/AgCl	I_{corr} (μA/cm²)	β_a (mV/dec)	β_c (mV/dec)	
0	0	0	−323.4	13.00	228	794	–
20	20	0	−350.0	4.43	197	487	65.92
20	0	30	−398.5	6.55	308	537	49.61
0	20	30	−374.2	8.13	223	434	37.46
20	20	30	−443.1	1.35	194	274	89.61

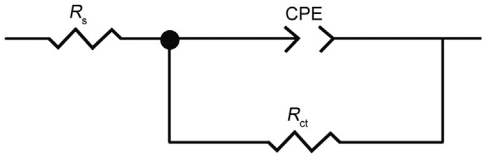

Fig. 6 Equivalent circuit used to fit the impedance data.

capacitance values and ascribed them due to the existence of a layer of the inner corrosion products.

In the present study, the control solution resulted in a slightly depressed semicircle with an R_{ct} value of 2575 Ω. When all the possible binary combinations are studied, significant increase in R_{ct} is observed only for the combination of phosphonate and zinc ions, while it is decreased for the mixture of phosphonate and LBA. The effect of the combination of zinc ions and LBA on R_{ct} is almost negligible. It indicates that among all the binary combinations, only phosphonate−Zn^{2+} is effective for corrosion control. This observation is due to the fact that phosphonate−Zn^{2+} combinations can synergistically control corrosion of carbon steel[1−7]. Low inhibition efficiency of 43% achieved by this combination is due to insufficient concentrations of both the components. When the concentrations of both the components are doubled to 40 mg L^{-1}, the inhibition efficiency is increased to 74%[13]. Interestingly, such high inhibition efficiency is also achieved by the addition of 30 mg L^{-1} of LBA to the binary combination of only 20 mg L^{-1} each of PBTC and Zn^{2+}. In the presence of this ternary inhibitor system, the R_{ct} value is increased enormously to 8635 Ω. This result indicates that the charge transfer resistance becomes dominant in the corrosion processes due to the presence of protective film on the metal surface. This inference is supported by the significant decrease in CPE and an increase in n value in the presence of the ternary inhibitor system. The CPE value at the metal/solution interface is found to decrease from 13.41 μF/cm^2 in the case of the control to 6.05 μF/cm^2. This is because of the replacement of water molecules in the electrical double layer by the organic molecules having low dielectric constants[38]. The value of n is considerably increased to 0.976 in the presence of the ternary inhibitor system suggesting the decrease of inhomogeneity of the interface during inhibition. These results indicate that there is formation of a protective film in the presence of the ternary inhibitor formulation. The inhibition efficiency obtained from impedance studies for 1 h immersion period is found to be 70.18%. Several authors, who studied the inhibitory effects of phosphonate-based corrosion inhibitors, also reported that there is formation of thick

Table 3 Impedance parameters for carbon steel in 200 mg L^{-1} NaCl environment in the absence and presence of inhibitor formulations

Concentration (mg L^{-1})			Impedance parameters			Inhibition efficiency, IE_i (%)
PBTC	Zn^{2+}	LBA	Charge transfer resistance, R_{ct} (Ω cm^2)	Constant phase element, CPE (μF/cm^2)	n	
0	0	0	2575	13.41	0.592	−
20	20	0	4555	10.79	0.676	43.47
20	0	30	2277	8.52	0.612	−13.09
0	20	30	2701	10.53	0.548	4.66
20	20	30	8635	6.05	0.776	70.18

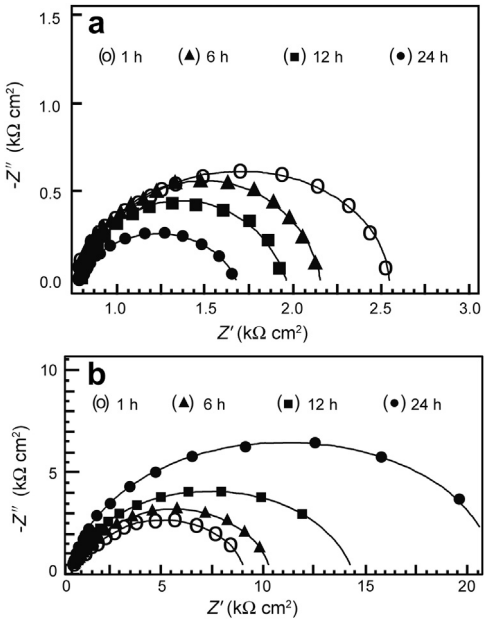

Fig. 7 Nyquist plots for carbon steel in the absence and presence of inhibitor at various immersion periods: (a) control; (b) inhibitor system.

and less permeable protective film on the metal surface[7,8,23]. They also concluded that the protective film consists of phosphonate-metal complexes. The impedance results obtained in the present study also infer the synergistic action operating between PBTC, Zn^{2+} and LBA. This inference is in agreement with those drawn from polarization and gravimetric studies.

A significant observation related to the inhibition efficiencies is to be noted. If the inhibition efficiencies obtained from gravimetric (IE_g), polarization (IE_p) and EIS (IE_i) studies are compared, slight differences are observed. For instance, the IE values obtained from gravimetric, polarization and impedance studies in the case of the ternary inhibitor system are 96%, 89% and 70%, respectively. It is suggested that the inhibition efficiencies obtained from various methods may not be strictly compared as the immersion time considered for all these methods is not the same.

3.3.2. Effect of immersion time. Nyquist plots for carbon steel in the control in the absence and presence of the ternary inhibitor formulation at different immersion periods (1−24 h) and at a constant temperature of 30 °C are shown in Fig. 7. The impedance parameters obtained from these plots and the inhibition efficiencies calculated from R_{ct} values are shown in Table 4. All the Nyquist plots are depressed capacitive loops, which are characterised by single time constant. In the case of the control, there is a slight decrease in R_{ct} with immersion period, while CPE is considerably increased to an extent of 9.79 μF/cm^2 after an immersion time of 24 h. The value of n ranges between 0.592 and 0.774. The significant increase in CPE is due to a large increase in the specific area caused by the presence of corrosion products on the metallic surface with time[37]. In the case of the ternary inhibitor formulation, there is an increase of R_{ct} value and decrease in CPE with increase in immersion time. The decrease in CPE may be due to the displacement of hydrated layer at the double layer by the developing inhibitor film on the surface[39]. Supposing that the electrochemical processes take place only at the pores and

Table 4 Impedance parameters for carbon steel in 200 mg L^{-1} NaCl environment in the absence and presence of the binary as well as ternary inhibitor formulations at different immersion periods and at a constant temperature of 30 °C

Immersion time	Impedance parameters			IE (%)
	R_{ct} (Ω cm^2)	CPE (μF/cm^2)	n	
Control − 200 mg L^{-1} NaCl				
1 h	2575	13.41	0.592	−
6 h	2080	16.85	0.613	−
12 h	1870	18.27	0.574	−
24 h	1598	23.20	0.658	−
Inhibitor formulation − PBTC (20 mg L^{-1}) + Zn^{2+} (20 mg L^{-1}) + LBA (30 mg L^{-1})				
1 h	8635	6.05	0.776	70.18
6 h	10,580	4.90	0.812	80.34
12 h	14,260	4.55	0.856	86.89
24 h	21,770	3.88	0.806	92.66

pinholes of the surface film, the increasing R_{ct} values give direct information on the growth and quality of the inhibitor film. Thus, these observations indicate that a continuous build up of inhibitor film is taking place with time resulting in the formation of a protective layer at the surface. In the case of the inhibitor formulation, the values of n at various immersion periods are close to each other, which infer that the homogeneity of the surface film is maintained during the immersion period studied. The inhibitor film formed after an immersion period of 24 h by all the three components of the ternary inhibitor formulation resulted in the rapid fall in the iron dissolution rate of the substrate, as indicated by its highest inhibition efficiency of 92.66%. From these studies, it may be noted that this highest inhibition efficiency, achieved after an immersion time of 24 h, is close to that obtained by gravimetric measurements. It is inferred that an immersion time of 24 h is required for the formation of the protective film.

3.3.3. Effect of temperature. Fig. 8 presents the Nyquist plots for carbon steel in the control in the absence and presence of the ternary inhibitor formulation at different temperatures. The impedance parameters obtained from these plots and the inhibition efficiencies calculated from R_{ct} values are shown in Table 5. All the Nyquist plots are depressed capacitive loops, which are characterized by single time constant. In the case of the control, there is a slight decrease in R_{ct} and an increase in CPE with temperature. The value of n is decreased from 0.758 at 30 °C to 0.687 at 60 °C. It is obvious that these changes are due to enhanced corrosion reactions at both the anodic and cathodic sites with increasing temperature in the absence of any inhibitor. It can be observed that in the case of the inhibitor formulation, the size of the capacitive loop is gradually decreased with increasing temperature. In the presence of the inhibitor system, the decrease in R_{ct} value is almost gradual with temperature and CPE is increased with temperature from 30 to 40 °C and later it is almost constant at further elevated temperatures. In the presence of the inhibitor formulation, the value of n decreased from 0.906 to 0.813. These observations can be attributed to the slight dissolution at the local areas of the protective film already present on the surface, making it slightly porous and inhomogeneous. It may also be due to desorption of some of the adsorbed inhibitor species at relatively higher temperatures. However, the inhibition efficiency is 87.67% even at 60 °C. Hence, it can be concluded that this ternary inhibitor system is efficient in the corrosion control of carbon steel at elevated temperatures even up to 60 °C.

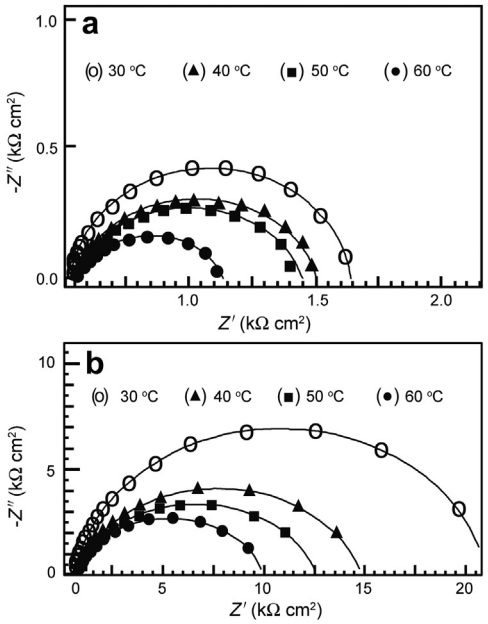

Fig. 8 Nyquist plots for carbon steel in the absence and presence of inhibitor at various temperatures: (a) control; (b) inhibitor system.

3.4. X-ray photoelectron spectroscopic studies

The X-ray photoelectron spectroscopic (XPS) deconvolution spectra of the individual elements present in the surface films in the absence and presence of inhibitor, PBTC (20 mg L^{-1}) + Zn^{2+} (20 mg L^{-1}) + LBA (30 mg L^{-1}), are shown in Figs. 9−13. The interpretation of all these spectra is done with the help of the data of the elemental binding energies reported in literature and also with the help of the reports published on the analysis of XPS spectra of the surface films.

The Fe 2*p* deconvolution spectrum in the case of the control is shown in Fig. 9(a). Two peaks are observed, one at 710.8 eV

Table 5 Impedance parameters for carbon steel in 200 mg L^{-1} NaCl environment in the absence and presence of the binary as well as ternary inhibitor formulations at different temperatures and constant immersion period of 1 h

Temperature	Impedance parameters			IE (%)
	R_{ct} (Ω cm^2)	CPE (μF/cm^2)	n	
Control − 200 mg L^{-1} NaCl				
30 °C	1598	23.20	0.658	−
40 °C	1494	25.90	0.440	−
50 °C	1446	29.40	0.262	−
60 °C	1198	30.90	0.149	−
Inhibitor formulation − PBTC (20 mg L^{-1}) + Zn^{2+} (20 mg L^{-1}) + LBA (30 mg L^{-1})				
30 °C	21,770	3.88	0.806	92.66
40 °C	14,600	5.78	0.761	89.77
50 °C	12,430	6.37	0.752	88.37
60 °C	9720	6.55	0.613	87.67

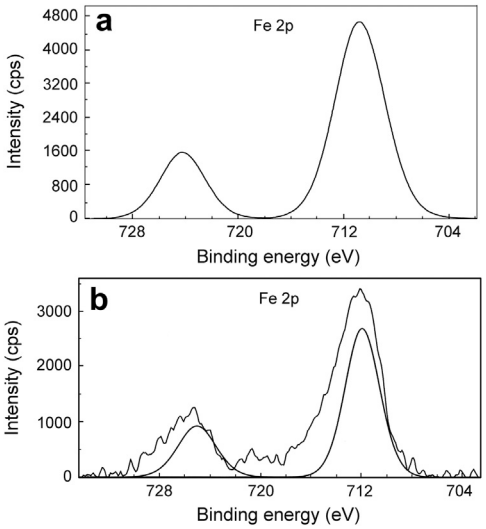

Fig. 9 XPS deconvolution spectra of Fe 2*p* in the surface films: (a) control; (b) inhibitor system.

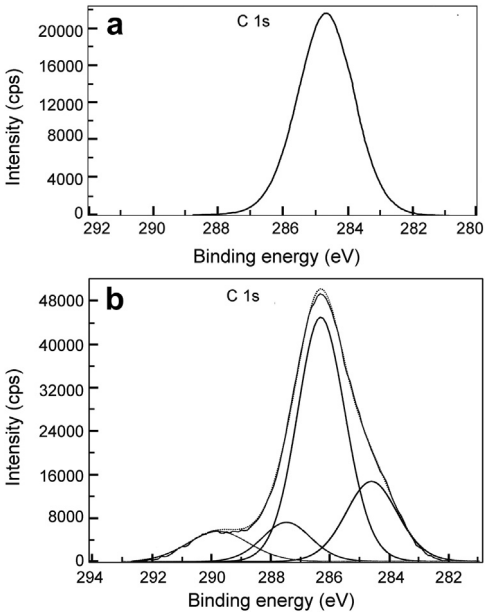

Fig. 11 XPS deconvolution spectra of C 1*s* in the surface films: (a) control; (b) inhibitor system.

corresponding to Fe $2p_{3/2}$ and the other one at 724.2 eV corresponding to Fe $2p_{1/2}$ electron. The peak due to Fe $2p_{3/2}$ is interpreted for the determination of chemical state of iron in the surface film. The peak of Fe $2p_{3/2}$ at 710.8 eV is the one, shifted from 707.0 eV, the characteristic elemental binding energy of Fe $2p_{3/2}$ electron[40]. Such a large shift of 3.8 eV suggests that iron is present in Fe^{3+} state in the surface film. The presence of a peak due to Fe $2p_{3/2}$ observed in the case of the control at 710.8 eV can be ascribed due to the presence of iron in the form of γ-Fe_2O_3, Fe_3O_4 and FeOOH[23,41−43]. In the case of the inhibitor system, the XPS (Fig. 9(b)) shows a single peak of Fe $2p_{3/2}$ at 712.0 eV. This peak at relatively higher binding energy may be due to Fe^{3+} involved in the complex formation with both PBTC and LBA. No peak is observed due to elemental iron in the case of control or inhibitor formulation. This result infers the formation of thick films in both the cases. The film is non-protective in the case of control and highly protective in the presence of inhibitor molecules. If the intensities of Fe $2p_{3/2}$ peaks are compared, they are 4600 cps for control and only 2600 cps for the inhibitor system. Such a decrease in the intensity of Fe 2*p* peak in the presence of the inhibitor can be understood because of the formation of protective film and consequently less corrosion of iron and less amount of iron oxide. The binding energy of Fe^{2+} state in iron oxides is reported to be around 708.5 eV[44]. The absence of any peak in this region in the present study also supports that iron does not exist in Fe^{2+} state.

The XPS spectrum of phosphorus, presented in Fig. 10, shows a single peak of P 2*p* at 133.8 eV. In the literature[45,46], it was reported that the P 2*p* peak could be observed in the range of 132.9−133.8 eV, for iron or steels immersed in the solutions containing phosphonates, orthophosphates and polyphosphates. Nakayama obtained a P 2*p* peak at 133.0 eV and attributed it to the presence of phosphonate compounds[47]. Felhosi et al. observed a P 2*p* peak at 132.1 eV in the XPS of the surface film

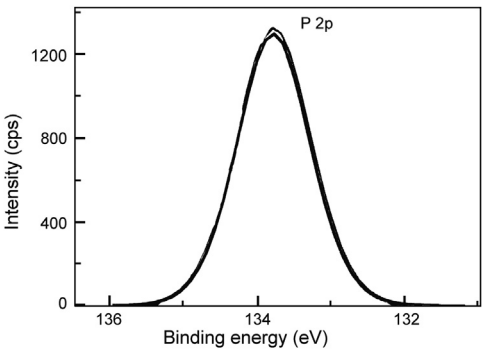

Fig. 10 XPS deconvolution spectrum of P 2*p* in the surface film formed in presence of the inhibitor system.

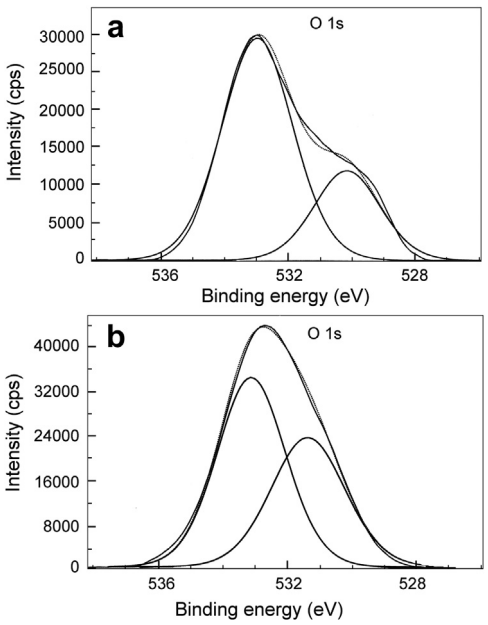

Fig. 12 XPS deconvolution spectra of O 1*s* in the surface films: (a) control; (b) inhibitor system.

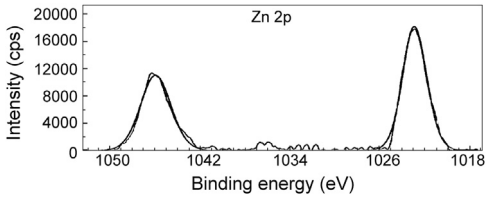

Fig. 13 XPS deconvolution spectrum of Zn 2*p* in the surface film formed in presence of the inhibitor system.

formed on carbon steel when immersed in a solution containing Zn^{2+} and HEDP[7]. They interpreted this peak due to the presence of [Zn−HEDP] complex in the surface film. Ochoa et al. in their studies on the mixtures of salts of phosphonocarboxylic acids and fatty amines as inhibitors for corrosion of carbon steel reported the P 2*p* peak at 132.1 eV and interpreted it due to the presence of phosphonate group in the surface film[48]. In the light of these reports, the P 2*p* peak observed in the present study suggests the presence of PBTC in the surface film formed in the case of the inhibitor.

The XPS spectra of C 1*s* are shown in Fig. 11. C 1*s* spectrum in the case of the control shows a single peak at 284.6 eV. This peak is due to contamination from the vacuum system and chamber during the analysis[49]. In the case of the inhibitor formulation, relatively more intense peak was observed at 286.3 eV along with three small peaks one each at 284.6 eV, 287.5 eV and 289.8 eV. Both PBTC and LBA have various carbon environments and formation of several peaks in the presence of the inhibitor formulation indicates that both PBTC and LBA ions are present in the surface film. Ochoa et al. in their studies on the mixtures of salts of phosphonocarboxylic acids and fatty amines as inhibitors for corrosion of carbon steel reported the C 1*s* peak at 284.5 eV[48]. This signal was accounted for by the presence of the inhibitor molecules on the steel surface. Gunasekaran and Chauhan studied the corrosion inhibition of mild steel by a plant extract and they obtained C 1*s* peaks at 285, 287 and 288.6 eV[30]. They interpreted these peaks due to C−C, C−O and CO bonds because of the organic molecules present in the plant extract. Aramaki and Shimura obtained a peak of organic carbon at 284.5 eV and they inferred that it is due to adsorbed organic inhibitor molecules on the surface[50].

The XPS spectra of O 1*s* are presented in Fig. 12. In the case of the control (Fig. 12(a)), two peaks corresponding to O 1*s* are observed, one of which is at 530.1 eV and the other one at 533.0 eV. The latter peak is essentially due to the adsorbed water on the surface[44,47,51]. Ochoa et al. obtained O 1*s* peak at 533.2 eV and attributed it to the presence of water molecules adsorbed on the oxide/hydroxide mixture[48]. In the present study, O 1*s* peak observed at 530.1 eV in the case of the control is due to O^{2-} [23,51], which may be in the form of oxides/hydroxides of Fe(III). In the case of the inhibitor formulation (Fig. 12(b)), two peaks are observed, one of which is at 533.2 eV and the other one at 531.4 eV. Fang et al. ascribed the O 1*s* peak observed at 531.3 eV to the complex formed between iron and phosphonate[52]. Pech-Canul and Bartolo-Perez observed the O 1*s* peak at 531.3 eV, which was ascribed to OH^- from hydrous iron oxides and to the complex formed between iron and phosphonate group[23]. It was also mentioned in their paper that such hydrous ferric oxides consist of $Fe(OH)_3$ and FeOOH. Felhosi et al. studied effects of bivalent cations on corrosion inhibition of steel by HEDP[7]. They mentioned that the O 1*s* peak at 531.4 eV is due to Fe−OH bond. Asami et al. observed O 1*s* peak at 531.5 eV in their study and attributed it to oxygen with a kind of Fe−O−H bond[44]. In light of these results and interpretations reported in literature, the O 1*s* peaks of high intensity observed in the present study may be interpreted as follows. The XPS of the surface film in presence of the inhibitor formulation shows that besides oxygen, there is presence of carbon, phosphorus, iron and zinc in the surface film. It shows that PBTC is present on the surface, zinc is present as Zn^{2+} and the interpretation given above in the case of Fe 2*p* indicates the presence of Fe_2O_3, Fe_3O_4 and FeOOH. Hence, O 1*s* peaks can be ascribed to the presence of $Zn(OH)_2$, Fe_2O_3, Fe_3O_4, FeOOH and oxygen of PBTC as well as LBA in the surface film. A comparison of intensities of O 1*s* peak in the control and in the presence of inhibitor system is of interest. In comparison to the intensity of 29,500 cps in control, the intensity of O 1*s* peak increases to 44,000 cps in the presence of inhibitor system. This increase is to be considered along with the high intensity of zinc (Fig. 13), of carbon (Fig. 11(b)) and of phosphorus (Fig. 10). The intensity of O 1*s* peak is related mainly to oxygen in one phosphonate and three carboxylate groups of PBTC, −OH groups of LBA and of $Zn(OH)_2$ and to small amounts of oxides/hydroxides of iron.

Fig. 13 presents the XPS deconvolution spectrum of zinc, with the Zn $2p_{3/2}$ peak at 1022.9 eV and the Zn $2p_{1/2}$ peak at 1046.0 eV. Zn $2p_{3/2}$ peak is normally interpreted. The high intensities of the Zn $2p_{3/2}$ peak may be ascribed to the presence of $Zn(OH)_2$ in the surface film and also to the involvement of Zn^{2+} in the complex formation with PBTC and LBA. It was reported in literature by Aramaki[53] that the Zn $2p_{3/2}$ peak at 1022.7 eV was due to the presence of $Zn(OH)_2$ in the surface film. Felhosi et al.[7] interpreted from the XPS analysis that there is formation of [Zn−HEDP] complex on the mild steel surface when it was immersed in a solution consisting of a mixture of HEDP and Zn^{2+}.

Along with the elements discussed above, the survey spectrum (not shown) in the case of the control has a low intensity chlorine peak at 200.0 eV. This is because some chloride ions reach the metal surface and are responsible for corrosion of the metal. The absence of chlorine peak in the survey spectrum of inhibited surface film indicates that the protective film does not allow the aggressive ions to reach the metal surface. After consolidating all the inferences drawn from the XPS of individual elements present in surface films, it is suggested that the surface film consists of mainly [Zn(II)−PBTC−LBA] complex, $Zn(OH)_2$ and small amounts of oxides/hydroxides of Fe(III) in the case of the inhibitor system. The complex may be chemisorbed on the metal surface and get attached to the Fe(III) ions.

3.5. Interpretation of FTIR spectra

The reflection absorption FTIR spectra of the surface films formed on carbon steel in the absence and presence of the inhibitor formulation, PBTC (20 mg L^{-1}) + Zn^{2+} (20 mg L^{-1}) + LBA (30 mg L^{-1}), are shown in Fig. 14. These spectra are interpreted in comparison to the FTIR spectra of pure PBTC and pure lactobionic acid (not shown here) as well as with the help of literature reports. In the FTIR spectrum of PBTC, multiple bands in the region, 900−1150 cm^{-1} were assigned to $-PO_3$ stretching frequencies[54]. The peak at 1200 cm^{-1} was assigned to PO group while the peak at 926 cm^{-1} was assigned to P−OH group[55,56]. In the case of the inhibited surface film in the present study, the peak due to PO is shifted from 1200 cm^{-1}

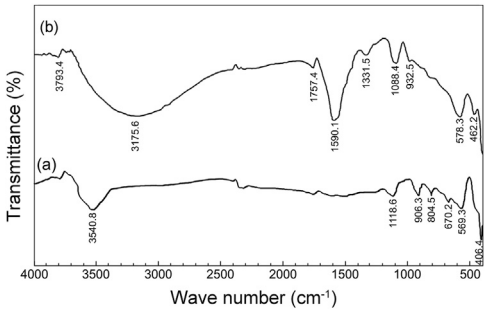

Fig. 14 Reflection absorption FTIR spectra of the surface films: (a) control; (b) inhibitor system.

to 1088.4 cm^{-1}. The P−OH stretching located at 932.5 cm^{-1} in the case of the formulation is observed to be weak. These results can be interpreted in terms of interaction between $P-O^-$ present in the phosphonate with metallic species, viz., Zn(II) and Fe(III) to form P−O−Zn and P−O−Fe bonds[8,57]. Carter et al. found that FTIR spectra obtained with an organic phosphonate on a steel substrate are consistent with the phosphonate reaction on steel to produce a metal salt[58]. This also suggests that phosphonates are coordinated with metal ions resulting in the formation of [metal−phosphonate] complexes on the metal surface.

Weak band observed at 1331.5 cm^{-1} (Fig. 14(b)) indicates the presence of zinc hydroxide in the surface film[2,4,57]. A very broad and intense band around 1716 cm^{-1} in the FTIR spectrum of PBTC was reported[59]. This is characteristic of uncoordinated, protonated carboxylate and was assigned to the CO stretch of −COOH. In the FTIR spectrum of pure lactobionic acid, the CO stretching frequency is observed at 1744.0 cm^{-1}. The small peak at 1757.4 cm^{-1} and an intense peak at 1590.1 cm^{-1} in the reflection absorption FTIR spectrum of the surface film in the case of the inhibitor system correspond to CO of both PBTC and LBA in the surface film. The shifts in the stretching frequency are resulted due to the involvement of these ions in the complex formation. There are several bands in the region, 1200−400 cm^{-1} in both the spectra of the surface films. Many of these peaks imply the presence of various oxides and hydroxides of iron like Fe_3O_4, FeOOH and Fe_2O_3[47,50,57,60]. A moderately intense and a broad band formed at 3540.8 cm^{-1}, in the case of the control, can be assigned to the presence of −OH group on the surface. This hydroxyl group may be in the form of FeOOH and/or $Fe(OH)_3$[61]. A very broad and intense band is observed near 3175.6 cm^{-1} in the case of the inhibitor formulation. This peak can be assigned to the −OH groups present in the inhibitor molecules, to $Zn(OH)_2$ and a small contribution of hydroxide of Fe(III) present in the inhibited film. Thus, the reflection absorption FTIR spectrum of the surface film formed in the presence of the inhibitor formulation infers the presence of [Zn(II)−PBTC−LBA] complex, $Zn(OH)_2$ and small amounts of oxides and hydroxides of Fe(III).

The XPS spectra and the reflection absorption FTIR spectrum of the surface film formed in the presence of the inhibitor formulation infer the presence of Fe(III), Zn(II), PBTC and LBA in the surface film. The shifts in binding energies of various elements and shifts in the absorption band frequencies of various functional groups infer that PBTC and LBA are involved in the complex formation with Zn^{2+} and Fe^{3+}. This inference is further

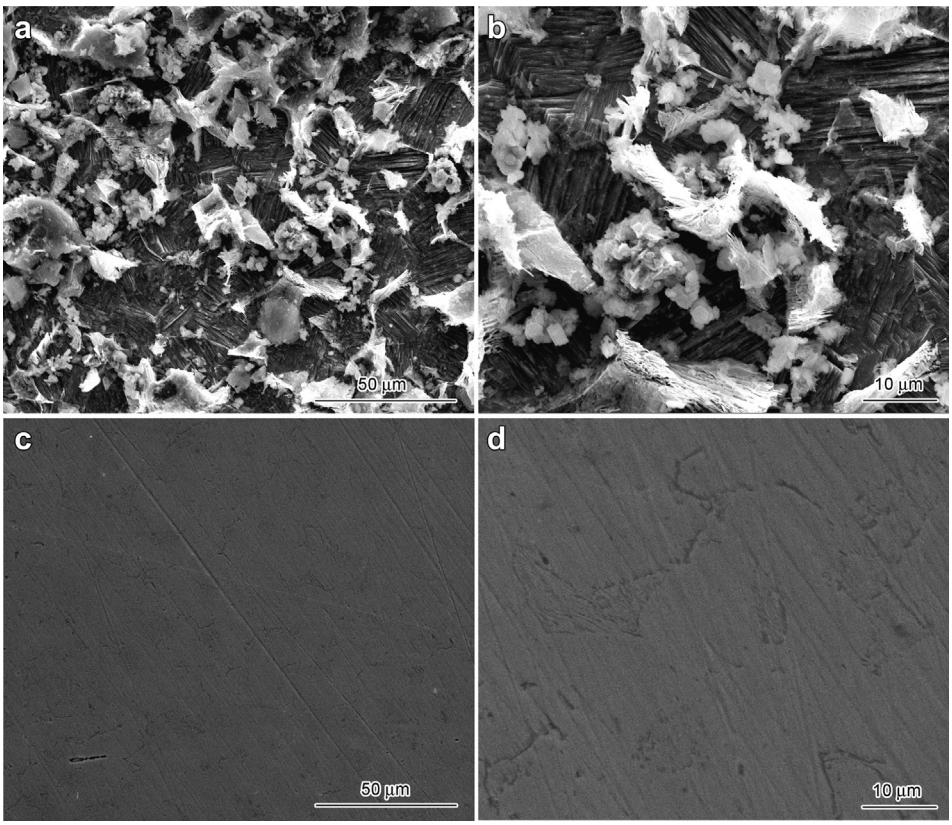

Fig. 15 High-resolution SEM images of carbon steel surfaces after immersion in control in the absence and presence of the inhibitor system: (a) and (b) control; (c) and (d) inhibitor system; (a) and (c) at low magnification; (b) and (d) at high magnification.

supported by several studies reported in literature[7,8,62−66]. Based on all these literature reports on various phosphonates and the requirement of optimum concentration of zinc ions for effective inhibition and also on the high intensity Zn 2*p* peaks obtained from XPS spectra, it can be inferred that Zn(II) and Fe(III) are involved in the complex formation with PBTC and LBA to form [Fe(III), Zn(II)−PBTC−LBA] polynuclear multi-ligand complex, which plays significant role in making the surface film protective.

3.6. Surface morphology by SEM

Fig. 15 shows the high-resolution SEM images of carbon steel surface immersed in control in the absence and presence of the inhibitor, PBTC (20 mg L^{-1}) + Zn^{2+} (20 mg L^{-1}) + LBA (30 mg L^{-1}). Fig. 15(a) indicates the severely corroded surface and the formation of different forms of corrosion products (iron oxides) on the surface in the absence of the inhibitor. The entire surface is covered by a scale-like black corrosion product, partially covered by corrosion product appearing in the form of white clusters. A very few of such clusters are shown at sub-micron level in Fig. 15(b). Fig. 15(c) and (d) shows the morphological features of the inhibited surface. The inhibited surface does not contain the corrosion products observed in the case of the control alone. Instead, the surface is completely covered by a uniform protective film. This film effectively controls the penetration of chloride ions of the environment onto the substrate. This observation also accounts for the high inhibition efficiencies obtained during the gravimetric studies of the inhibitor system. From the SEM analysis it can be inferred that the inhibitor film exhibits good protective properties for carbon steel in low chloride media.

3.7. Surface topography by AFM

AFM imaging gives a perspective of the "*Z*" direction with three dimensional images[67,68]. Fig. 16 shows the AFM topographical images of the surfaces of carbon steel immersed in the control in the absence and presence of the inhibitor formulation, PBTC (20 mg L^{-1}) + Zn^{2+} (20 mg L^{-1}) + LBA (30 mg L^{-1}). A severely corroded surface morphology (Fig. 16(a)) is observed after immersion in the control in the absence of the inhibitor. The root-mean-square (RMS) roughness is found to be 504 nm, which clearly indicates the high roughness of the corroded surface. The microstructure of the surface shows several smaller and larger corrosion product deposits. In the presence of the inhibitor, the surface is found to possess a homogeneous topography (Fig. 16(b)) with low dispersion in height and without any predominant peak structure. The drastic decrease in RMS roughness from 504 nm in the case of the control to 8 nm observed in the case of the inhibitor, clearly infers the greater smoothness and homogeneity of the surface film produced by the inhibitor formulation and the absence of any corrosion product deposits. The results of the surface topographical studies strongly support the inferences drawn above in the gravimetric and electrochemical studies, in favour of the protective nature of the surface film produced by the inhibitor formulation.

3.8. Mechanism of corrosion inhibition

In order to explain all the experimental results, a plausible mechanism of corrosion inhibition is proposed as follows:

(1) The mechanism of corrosion of carbon steel in nearly neutral aqueous media is well established. The well-known reactions are mentioned below.

$$Fe \rightarrow Fe^{2+} + 2e^{-} \quad (5)$$

Fe^{2+} further undergoes oxidation in the presence of oxygen available in the aqueous solution.

$$Fe^{2+} \xrightarrow{[O_2]} Fe^{3+} + e^{-} \quad (6)$$

(2) The corresponding reduction reaction at cathodic sites in neutral and alkaline media is

$$O_2 + 2H_2O + 4e^{-} \rightarrow 4OH^{-} \quad (7)$$

Fe^{3+} ions produced at anodic areas and OH^{-} ions produced at cathodic areas combine to form $Fe(OH)_3$, ($Fe_2O_3 \cdot H_2O$) which gets precipitated on the surface of the metal due to its very low solubility product.

(3) When PBTC, Zn^{2+} and LBA are added to the aqueous solution, both PBTC and LBA react with Zn^{2+} to form a ternary complex, [Zn^{2+}−PBTC−LBA]. This complex diffuses to the metal surface and binds with Fe(III) ions available on the metal surface. A dense polymeric network structure is constituted on the surface by high degree of

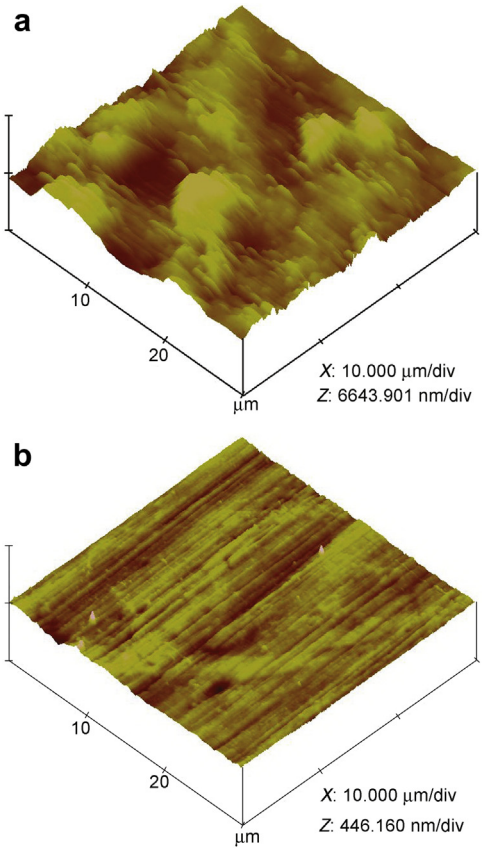

Fig. 16 AFM topographical images of carbon steel surfaces after immersion in control in the absence and presence of the inhibitor system: (a) control; (b) inhibitor system.

cross-linkage and reorganisation. The polynuclear multiligand complex, [Fe(III), Zn(II)−PBTC−LBA] covers the anodic sites and controls the anodic reaction of the corrosion process. Several recent reports on corrosion inhibition in various media inferred that the inhibitor molecules get adsorbed on the substrate surface and block the active corrosion sites[69−72]. Felhosi et al.[73] showed that iron can be passivated by simple immersion of it in aqueous solutions of 1,7-diphosphonoheptane. The formation of protective layer by the phosphonate consists of a fast adsorption step and subsequent slower process, which is supposed to be due to the organisation. According to the authors, this effect is due to the formation of self-assembling layer of complexes of the organic inhibitor with iron.

$$[\mathrm{Zn(II)-PBTC-LBA}]+\mathrm{Fe^{3+}}\rightarrow[\mathrm{Fe(III),Zn(II)-PBTC-LBA}] \quad (8)$$

(4) Free Zn^{2+} ions are available in the bulk of the solution because of relatively higher molar concentration of Zn^{2+} in the inhibitor mixture. These Zn^{2+} ions diffuse to the metal surface and react with OH^- ions produced at the cathodic sites to form a precipitate of $Zn(OH)_2$.

$$\mathrm{Zn^{2+}}+2\mathrm{OH^-}\rightarrow\mathrm{Zn(OH)_2} \quad (9)$$

The precipitate of $Zn(OH)_2$ gets deposited on the cathodic sites and controls the cathodic partial reaction of corrosion process.

(5) The decrease in inhibition efficiency when the bulk concentration of LBA is higher than the optimum value can be explained as follows. It may be noted that the molar ratio of Zn^{2+}:PBTC:LBA in the bulk of the solution is 4.13:1:2.64, when the inhibition efficiency is found to be very less. When the bulk concentration of LBA is higher, the nature and composition of the complex, [Zn(II)−PBTC−LBA] may be entirely different, with more LBA than PBTC. Such a complex may not be protective. Secondly, higher concentration of free LBA is available in the bulk of the solution. This free LBA diffuses to the steel surface and gets chemisorbed on the metal surface. To that extent, the protective [Zn(II)−PBTC−LBA] complex will not be available on the metal surface.

(6) The ternary inhibitor formulation is effective in the pH range, 5−8. At pH 9, higher concentration of OH^- ions are available both in the bulk of the solution and on the surface. In such an environment, there is greater interference of OH^- ions in the complexation[74] leading to the formation of [Zn(II)−PBTC−LBA−OH] complex, which may not contribute to the formation of protective film on the metal surface. In acidic medium at pH 4, the ligands will be in the protonated form and do not coordinate with Zn(II) as effectively as the deprotonated ligands. Secondly, enough amount of $Zn(OH)_2$ will not be formed on the cathodic sites. Hence, at pH 4 the decrease in inhibition efficiency is observed.

(7) Thus, PBTC, Zn^{2+} and LBA play a very important role in the synergistic effect in controlling corrosion through the formation of protective film on the metal surface. It is inferred that the film may consist of various oxides/hydroxides like Fe_2O_3, $Fe_3O_4\cdot H_2O$, FeOOH, $Zn(OH)_2$ and a polynuclear multiligand complex, [Fe(III), Zn(II)−PBTC−LBA]. Each of these constituents contributes itself to make the film highly protective.

4. Conclusions

(1) Lactobionic acid, a non-toxic organic compound is proved to be an excellent synergist in combination with PBTC and Zn^{2+} for corrosion control of carbon steel in nearly neutral aqueous environment.

(2) The ternary formulation containing 20 mg L^{-1} each of PBTC and Zn^{2+} along with 30 mg L^{-1} of lactobionate is an effective corrosion inhibitor for carbon steel. Once the protective film is formed, a mixture of only 10 mg L^{-1} each of PBTC and Zn^{2+} and 20 mg L^{-1} of lactobionate will serve as the maintenance dosage. The ternary inhibitor system is thus relatively more environmentally friendly.

(3) The inhibitor system is effective in the pH range 5−8.

(4) The inhibitor formulation acts as a mixed type inhibitor controlling both the anodic and cathodic reactions.

(5) Significant modification of the metal/solution interface occurs through the formation of dense protective film in the presence of the inhibitor formulation.

(6) The formation of protective film on the metal surface requires 24 h immersion time.

(7) The inhibitor formulation affords good inhibition efficiency even at a higher temperature of 60 °C.

(8) The protective film consists of mainly [Zn(II)−PBTC−lactobionate] complex, $Zn(OH)_2$ and small amounts of oxides/hydroxides of Fe(III). Presence of optimum amounts of all these compounds is required at a given pH value to make the surface film protective.

REFERENCES

[1] J. Telegdi, M.M. Shaglouf, A. Shaban, F.H. Karman, I. Betroti, M. Mohai, E. Kalman, Electrochim. Acta 46 (2001) 3791−3799.
[2] G. Gunasekaran, N. Palaniswamy, B.V. Appa Rao, V.S. Muralidharan, Electrochim. Acta 42 (1997) 1427−1434.
[3] S. Rajendran, B.V. Appa Rao, N. Palaniswamy, Electrochim. Acta 44 (1998) 533−537.
[4] I. Sekine, Y. Hirakawa, Corrosion 42 (1986) 272−277.
[5] H.S. Awad, Corros. Eng. Sci. Tech. 40 (2005) 57−64.
[6] Y. Gonzalez, M.C. Lafont, N. Pebere, G. Chatainier, J. Roy, T. Bouissou, Corros. Sci. 37 (1995) 1823−1837.
[7] I. Felhosi, Zs. Keresztes, F.H. Karman, M. Mohai, I. Bertoti, E. Kalman, J. Electrochem. Soc. 146 (1999) 961−969.
[8] Y. Gonzalez, M.C. Lafont, N. Pebere, F. Moran, J. Appl. Electrochem. 26 (1996) 1259−1265.
[9] E. Kalman. Ann. Univ. Ferrara, N.S., Sez. V, in: Proceedings to the 7th European Symposium on Corrosion Inhibitors (7SEIC), 1990, p. 745.
[10] G. Gunasekaran, R. Natarajan, N. Palaniswamy, Corros. Sci. 43 (2001) 1615−1626.
[11] B.V. Appa Rao, S. Srinivasa Rao, M. Venkateswara Rao, Corros. Eng. Sci. Tech. 43 (2008) 46−53.
[12] G. Gunasekaran, R. Natarajan, B.V. Appa Rao, N. Palaniswamy, V.S. Muralidharan, Indian J. Chem. Technol. 5 (1998) 91−94.
[13] B.V. Appa Rao, S. Srinivasa Rao, Mater. Corros. 61 (2010) 285−301.

[14] RPA Report J480bNon Surfactant Organic Ingredients and Zeolite-based Detergents, Scientific Committee on Health and Environmental Risks − European Commission, 2006.
[15] G. Bohnsack, K.H. Lee, D.A. Johnson, E. Buss, Mater. Perform. 25 (1986) 32−39.
[16] K.G. Gerling, in: Proceedings to the 2nd International Whey Conference, International Dairy Federation, Chicago, Illinois, 1998, p. 251.
[17] Graciela M. Escandar, Alejandro C. Olivieri, Manuel Gonzalez-Sierra, Luis F. Sala, J. Chem. Soc. Dalton Trans. (1994) 1189−1192.
[18] ASTM Standard G 31-72'Standard Practice for Laboratory Immersion Corrosion Testing of Materials' (Reapproved 1990), Annual Book of ASTM Standards, vol. 0302, ASTM, Philadelphia, PA, 1990.
[19] R.A. Freeman, D.C. Silverman, Corrosion 48 (1992) 463−466.
[20] M. Elachouri, M.S. Hajju, M. Salem, S. Kertit, J. Aride, R. Coudert, E. Essassi, Corrosion 52 (1996) 103−108.
[21] Alejandro A. Frutos, Graciela M. Escandar, Juan Manuel Salas Peregrin, Manuel Gonzalez Sierra, Luis F. Sala, Can. J. Chem. 75 (1997) 405−413.
[22] D. Gopi, S. Manimozhi, K.M. Govindaraju, P. Manisankar, S. Rajeswari, J. Appl. Electrochem. 37 (2007) 439−449.
[23] M.A. Pech-Canul, P. Bartolo-Perez, Surf. Coat. Technol. 184 (2004) 133−140.
[24] S. Rajendran, B.V. Appa Rao, N. Palaniswamy, Anti-Corros. Methods Mater. 46 (1999) 23−28.
[25] R.S. Goncalves, D.S. Azambuja, A.M. Serpa Lucho, Corros. Sci. 44 (2002) 467−479.
[26] F. Mansfeld, M.W. Kendig, W.J. Lorenz, J. Electrochem. Soc. 132 (1985) 290−296.
[27] F. Mansfeld, M.W. Kendig, Werkst. Korros. 34 (1983) 397−401.
[28] R. Macdonald, D.R. Franceschetti, Impedance Spectroscopy, J.R. Macdonald (Ed.), Wiley, New York, 1987, pp. 96.
[29] D.A. Lopez, S.N. Simison, S.R. de Sanchez, Electrochim. Acta 48 (2003) 845−854.
[30] G. Gunasekaran, L.R. Chauhan, Electrochim. Acta 49 (2004) 4387−4395.
[31] M.S. Morad, Corros. Sci. 42 (2000) 1307−1326.
[32] A. Alagta, I. Felhosi, J. Telegdi, I. Bertoti, E. Kalman, Corros. Sci. 49 (2007) 2754−2766.
[33] Najoua Labjar, Mounim Lebrini, Fouad Bentiss, Nour-Eddine Chihib, Souad El Hajjaji, Charafeddine Jama, Mater. Chem. Phys. 119 (2010) 330−336.
[34] K. Babic-Samardzija, C. Lupu, N. Hackerman, A.R. Barron, A. Luttge, Langmuir 21 (2005) 12187−12196.
[35] K.F. Khaled, Electrochim. Acta 48 (2003) 2493−2503.
[36] E. Machnikova, Kenton H. Whitmire, N. Hackerman, Electrochim. Acta 53 (2008) 6024−6032.
[37] A. Bonnel, F. Dabosi, C. Deslovis, M. Duprat, M. Keddam, B. Tribollet, J. Electrochem. Soc. 130 (1983) 753−761.
[38] C.T. Wang, S.H. Chen, H.Y. Ma, L. Hua, N.X. Wang, J. Serb. Chem. Soc. 67 (2002) 685−696.
[39] I. Felhosi, J. Telegdi, G. Palinkas, E. Kalman, Electrochim. Acta 47 (2002) 2335−2340.
[40] J.F. Moulder, W.F. Stickle, P.E. Sobol, K.D. Bamben, Handbook of X-ray Photoelectron Spectroscopy, a Reference Book of Standard Spectra for Identification and Interpretation of XPS Data, Physical Electronics, USA, 1995.
[41] E. Kalman, F.H. Karman, I. Cserny, L. Kover, J. Telegdi, D. Varga, Electrochim. Acta 39 (1994) 1179−1182.
[42] N.S. Mc Intyre, D.G. Zetaruk, Anal. Chem. 49 (1977) 1521−1529.
[43] S. Maroie, M. Savy, J.J. Verbist, Inorg. Chem. 18 (1979) 2560−2567.
[44] K. Asami, K. Hashimoto, S. Shimodaira, Corros. Sci. 16 (1976) 35−45.
[45] M. Koudelka, J. Sanchez, J. Augustynski, J. Electrochem. Soc. 129 (1982) 1186−1191.
[46] B.E. Moriarty, in: Proceedings to the Corrosion 89, New Orleans Convention Center, New Orleans, Louisiana, 1989, p. 612.
[47] N. Nakayama, Corros. Sci. 42 (2000) 1897−1920.
[48] N. Ochoa, G. Baril, F. Moran, N. Pebere, J. Appl. Electrochem. 32 (2002) 497−504.
[49] G.P. Cicileo, B.M. Rosales, F.e. Varela, J.R. Vilche, Corros. Sci. 41 (1999) 1359−1375.
[50] K. Aramaki, T. Shimura, Corros. Sci. 45 (2003) 2639−2655.
[51] F.H. Karman, I. Felhosi, E. Kalman, I. Cserny, L. Kover, Electrochim. Acta 43 (1998) 69−75.
[52] J.L. Fang, Y. Li, X.R. Ye, Z.W. Wang, Q. Liu, Corrosion 49 (1993) 266−270.
[53] K. Aramaki, Corros. Sci. 45 (2003) 1085−1101.
[54] K.D. Demadis, S. Katarachia, Phosphorus Sulfur Silicon 179 (2004) 627−648.
[55] N.B. Colthup, L.H. Daly, S.E. Wiberley, Introduction to Infrared and Raman Spectroscopy, third ed., Academic Press, New York, 1990.
[56] K. Nakamoto, Infrared and Raman Spectra of Inorganic and Coordination Compounds, fourth ed., John Wiley & Sons, New York, 1986.
[57] H. Amar, J. Benzakour, A. Derja, D. Villemin, B. Moreau, T. Braisaz, A. Tounsi, Corros. Sci. 50 (2008) 124−130.
[58] R.O. Carter, C.A. Gierczak, R.A. Dickie, Appl. Spectrosc. 40 (1986) 649−655.
[59] K.D. Demadis, D. Coucouvanis, Inorg. Chem. 34 (1995) 436−448.
[60] S. Yu, G.M. Chow, J. Mater. Chem. 14 (2004) 2781−2786.
[61] L.J. Bellamy, Advances in Infrared Group Frequencies, The Chaucer Press Limited, Great Britain, 1968, p. 94.
[62] R. Holm, D. Holtkamp, R. Kleinstuck, H.-J. Rother, S. Storp, Z. Fresenius, Anal. Chem. 333 (1989) 546−554.
[63] J.-G. Mao, A. Clearfield, Inorg. Chem. 41 (2002) 2319−2324.
[64] Yu.I. Kuznetsov, in: Proceedings to the European Corrosion Congress (EUROCORR 2003), Budapest, Hungary, 2003, p. 320.
[65] A.J. Freedman, Mater. Perform. 23 (1984) 9−16.
[66] A. Shaban, E. Kalman, I. Biczo, Corros. Sci. 35 (1993) 1463−1470.
[67] N.M. Martyak, R. Seefeldt, Electrochim. Acta 49 (2004) 4303−4311.
[68] E. Barrera, M.P. Palomar, N. Batina, I. Gonzalez, J. Electrochem. Soc. 147 (2000) 1787−1796.
[69] Ali Reza Hosein Zadeh, Iman Danaee, Mohamad Hosein Maddahy, J. Mater. Sci. Technol. 29 (2013) 884−892.
[70] I. Danaee, M. Niknejad Khomami, A.A. Attar, J. Mater. Sci. Technol. 29 (2013) 89−96.
[71] Hong Ju, Yulin Ju, Yan Li, J. Mater. Sci. Technol. 28 (2012) 809−816.
[72] K.P. Vinod Kumar, M. Sankara Narayana Pillai, G. Rexin Thusnavis, J. Mater. Sci. Technol. 27 (2011) 1143−1149.
[73] I. Felhosi, E. Kalman, P. Poczik, Russ. J. Electrochem. 38 (2002) 230−237.
[74] V. Deluchat, J.-C. Bollinger, B. Serpaud, C. Caullet, Talanta 44 (1997) 897−907.